Inorganic Chemistry

Communication

pubs.acs.org/IC

Tuning of the Critical Temperature in Iron(II) Spin-Crossover Materials Based on Bridging Polycyanidometallates: Pentacyanidonitrosylferrate(II) and Hexacyanidoplatinate(IV)

Radovan Herchel,[†] Zdeněk Trávníček,*[,‡] and Radek Zbořil[§]

[†]Department of Inorganic Chemistry, [‡]Regional Centre of Advanced Technologies and Materials, Department of Inorganic Chemistry, and [§]Regional Centre of Advanced Technologies and Materials, Department of Physical Chemistry, Faculty of Science, Palacký University in Olomouc, 17 listopadu 12, CZ 771 46 Olomouc, Czech Republic

Supporting Information

ABSTRACT: The reactions of iron(II) sulfate, 4-amino-3,5-di-2-pyridyl-4*H*-1,2,4-triazole (abpt), and pentacyanidonitrosylferrate(II) or hexacyanidoplatinate-(IV) resulted in the formation of one-dimensional iron(II) spin-crossover compounds $[Fe(abpt)_2(\mu\text{-}Fe(CN)_5(NO))]_n$ (**1**) and $[Fe(abpt)_2(\mu\text{-}Pt(CN)_6)]_n$ (**2**) with the spin-transition critical temperature near or above room temperature accompanied by thermochromism. Furthermore, it has been proven that the critical temperature T_c is influenced by the type of dianionic polycyanidometallate within the series of discussed systems, and it changes in the sequence of $[Fe(CN)_5(NO)]^{2-} < [Pt(CN)_6]^{2-} < [Ni(CN)_4]^{2-} \approx [Pd(CN)_4]^{2-} \approx [Pt(CN)_4]^{2-}$.

Spin-crossover (SCO) is a fascinating phenomenon of molecular bistability in the field of molecular magnetism[1] and is mainly investigated for iron(II) coordination compounds. In such a case, the interplay between diamagnetic low-spin (LS) $t_{2g}^6e_g^0$ and paramagnetic high-spin (HS) $t_{2g}^4e_g^2$ octahedral electronic configurations is driven by external stimuli (e.g., temperature, pressure, and irradiation) and is often accompanied by thermochromism, piezochromism, and photochromism,[2] which can be utilized in the construction of molecular devices.[3] Furthermore, the frontiers of spin-transition research have recently been shifted toward "nano-world", revealing new applications.[4] Frequently, the metallocyanates $[M(CN)_x]^{y-}$ play an important role as building blocks in SCO coordination chemistry.[5] The number of cyanido ligands, *x*, and the total charge of the $[M(CN)_x]^{y-}$ moiety, *y*, may determine the final structural dimensionality of prepared compounds and, together with the nature of transition metal M^{x-y}, can significantly affect the SCO properties. There are many interesting SCO compounds employing dianionic metallocyanates, which are limited to square-planar tetracyanidometallates, such as $[M(CN)_4]^{2-}$ (M = Ni, Pd, Pt).[5a] Herein, we report on the first utilization of the pentacyanidonitrosylferrate-(II), $[Fe(CN)_5(NO)]^{2-}$, and hexacyanidoplatinate(IV), $[Pt(CN)_6)]^{2-}$, anions as octahedral bridging metallocyanates in iron(II) SCO chemistry. Pentacyanidonitrosylferrate(II) is widely used in coordination chemistry, but only one trinuclear compound, $[\{Fe^{III}(salpet)\}_2\{\mu\text{-}Fe(CN)_5NO\}]$, is known in which the iron(III) centers undergo spin transitions.[6] Surprisingly, the coordination chemistry of hexacyanidoplatinate(IV) is very poor in contrast to tetracyanidoplatinate(II) and is mostly limited to the $M^I_2[Pt(CN)_6)]$ and $M^{II}[Pt(CN)_6)]$ species.[7] The reported iron(II) coordination polymers $[Fe(abpt)_2(\mu\text{-}Fe(CN)_5(NO))]_n$ (**1**) and $[Fe(abpt)_2(\mu\text{-}Pt(CN)_6)]_n$ (**2**) were prepared by the reaction of $FeSO_4{\cdot}7H_2O$ and 4-amino-3,5-di-2-pyridyl-4*H*-1,2,4-triazole (abpt) with $Na_2[Fe(CN)_5NO]{\cdot}2H_2O$ or $K_2[Pt(CN)_6]$, respectively.[8] The composition and purity of complexes **1** and **2** were confirmed by elemental analysis, Fourier transform IR spectroscopy, and powder X-ray diffraction (PXRD). The single crystals of **1** suitable for XRD analysis were prepared by slow diffusion in silica gel.[8] Compound **1** revealed the one-dimensional (1D) chain structure in which the planar $[Fe(abpt)]^{2+}$ cations are bridged by pentacyanidonitrosylferrate(II) (Figure 1).

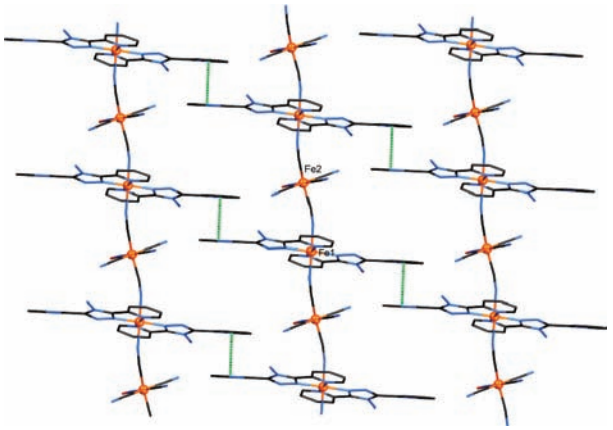

Figure 1. Part of the crystal structure of **1** showing the 1D chain motif and interchain $\pi-\pi$-stacking interactions (dashed lines). The hydrogen atoms are omitted for clarity.

Complex **1** crystallizes in the *P*1 space group, and its molecular structure including a labeling scheme is depicted in Figure S1 in the Supporting Information (SI). At 100 K, the Fe–N bond length interval of SCO affecting the iron center Fe1 with the $\{FeN_6\}$ chromophore is 1.953(4)–2.010(3) Å,

Received: August 5, 2011
Published: November 18, 2011

and it covers the interval found in abpt-containing iron(II) SCO compounds in the LS state.[9] There are two types of significant interchain noncovalent contacts: (i) the $\pi-\pi$-stacking interactions between the pyridyl rings of the abpt ligand with the centroid's distance equal to 3.5389(1) Å (Figure 1); (ii) the N−H···N hydrogen bonds between the amino group of abpt and cyanido ligands of pentacyanidonitrosylferrate (Figure S2 in the SI). These interactions are expanded into different directions, and as a result of this, the quasi-three-dimensional structure is formed. The polycrystalline samples also undergo thermochromism, which is demonstrated in Figure 2. Compound **1** changes color from dark brown at 77 K

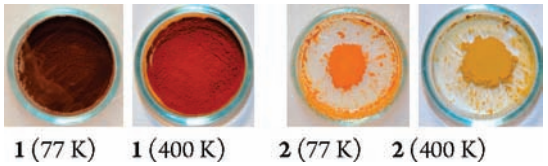

Figure 2. Pictures showing the thermochromism of compounds **1** and **2** at different temperatures.

to red at 400 K. Also, the orange color of **2** converts into yellowish brown upon heating.

The magnetic data of **1** and **2** were measured in the temperature interval of 5−400 K under an applied field of 1 T and are displayed in the form of molar susceptibilities and effective magnetic moments in Figure 3. For both compounds,

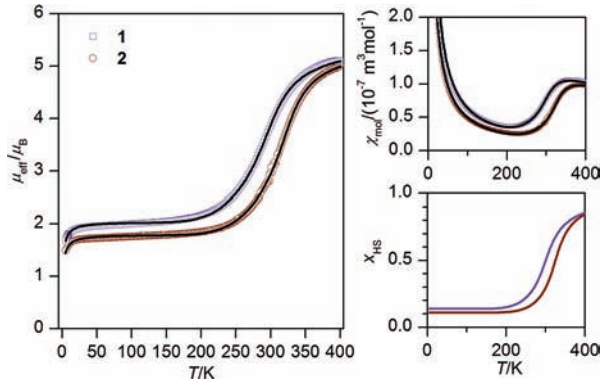

Figure 3. Temperature dependence of the effective magnetic moments, molar susceptibilities, and total HS molar fractions for **1** and **2**. Empty symbols: experimental data. Full lines: calculated data using a model and parameters listed in the text.

the magnetic susceptibility is monotonically decreasing upon heating and reaching its minimum at ca. 210 K. Afterward, an increase of the molar susceptibility is observed, which indicates the spin transition in **1** and **2**. The effective magnetic moments at lower temperature (≈50 K) reach plateaus of 1.96 μ_B for **1** and 1.73 μ_B for **2**. Because the LS iron(II) complexes are diamagnetic, these low-temperature nonzero susceptibilities and effective magnetic moments can be explained by the incomplete SCO and, hence, the occurrence of the HS iron(II) fraction. Similar incomplete SCOs were reported for two other 1D chains containing the abpt ligand, namely, $[Fe(abpt)_2(\mu\text{-tcpd})]_n$ ($tcpd^{2-}$ = $(C[C(CN)_2]_3)^{2-}$) and $[Fe(abpt)_2(\mu\text{-Ni}(CN)_4)]_n$, in which the residual HS fractions were 30% and 13%, respectively.[10] Upon heating, the gradual increase of the effective magnetic moments is observed above ca. 200 K and the final values of μ_{eff} are 5.10 μ_B for **1** and 5.01 μ_B for **2** at T = 400 K. The theoretical (spin-only) HS value of the effective magnetic moment for S = 2 is 4.90 μ_B (g = 2.0), but usually iron(II) has a g factor close to the value of 2.2,[11] which would result in μ_{eff} = 5.39 μ_B. Thus, we might presume that, even at such a high temperature, the SCO is not completed. It is worth mentioning that this magnetic behavior was reproducible also after several cycles of heating and cooling and also for different batches of compounds **1** and **2**. In order to quantitatively describe the SCO behavior of the compounds under study, an Ising-like model was used.[12] The three free parameters define the HS mole fraction x'_{HS} as a function of the temperature, and they are as follows: Δ = energy difference between the HS and LS states; γ = cooperativness; r_{eff} = effective degeneracy ratio between the HS and LS states. In the next step, the molar susceptibility is calculated as $\chi_{mol} = (x''_{HS} + x_{rHS})\chi_{HS} + (1 - x''_{HS} - x_{rHS})\chi_{LS}$, where x_{rHS} is the mole fraction of the residual HS state observed at low temperature and x''_{HS} is the rescaled HS fraction calculated from an Ising-like model as $x''_{HS} = x'_{HS}(1 - x_{rHS})$. The total HS mole fraction x_{HS} is then equal to $x_{HS} = x''_{HS} + x_{rHS}$ and is shown in Figure 3. The molar susceptibility of the HS state χ_{HS} was calculated using the Curie−Weiss equation, and χ_{LS} is equal to zero. Finally, the parameters Δ, γ, r_{eff}, x_{rHS}, g_{HS}, and Θ_{HS} were varied during the fitting procedure. The resulting parameters were g_{HS} = 2.25, Θ_{HS} = −2.5 K, x_{rHS} = 14%, Δ = 1287 K, r_{eff} = 79, and γ = 218 K for **1** and g_{HS} = 2.22, Θ_{HS} = −2.7 K, x_{rHS} = 11%, Δ = 1640 K, r_{eff} = 166, and γ = 234 K for **2**. The fitted g factors reveal the expected values for HS octahedral iron(II), and negative Weiss constants reflect the zero-field splitting of residual HS iron(II) centers and their possible intrachain interactions mediated by bridging metallocyanates. The calculated enthalpy and entropy of spin transition are ΔH = 10.7 kJ mol^{-1} and ΔS = 36.3 J K^{-1} mol^{-1} for **1** and ΔH = 13.6 kJ mol^{-1} and ΔS = 42.5 J K^{-1} mol^{-1} for **2**. These parameters adopt typical values for iron(II) SCO compounds. Estimated critical temperatures (T_c) based on the condition that x_{HS} = 0.5 are 300 K for **1** and 325 K for **2**. With the aim of more deeply understanding the SCO development in this class of coordination polymers, the transmission ^{57}Fe Mössbauer spectra were collected at different temperatures. In order to improve the signal-to-noise ratio and to simplify the analysis by suppressing the absorption of the nitroprusside anion, an isotopically enriched sample, $[^{57}Fe(abpt)_2(\mu\text{-Fe}(CN)_5(NO))]_n$ (**1′**), was used. First, the spectrum of **1′** measured at 25 K consists of four doublets with parameters of δ_1 = −0.20 mm s^{-1}, ΔE_{Q_1} = 1.68 mm s^{-1}, δ_2 = 0.52 mm s^{-1}, ΔE_{Q_2} = 0.48 mm s^{-1}, δ_3 = 1.13 mm s^{-1}, ΔE_{Q_3} = 3.74 mm s^{-1}, and δ_4 = 1.22 mm s^{-1}, ΔE_{Q_4} = 3.04 mm s^{-1} (Figure 4). The first doublet may be assigned to LS iron(II) of pentacyanidonitrosylferrate.[13] The second doublet corresponds to $[Fe(abpt)_2]^{2+}$ in the LS state. Finally, the third and fourth doublets correspond to $[Fe(abpt)_2]^{2+}$ in the HS state. The areas of the absorption peaks are in the ratio A_1:A_2:A_3:A_4 = 3.6:72:7.4:17 and, hence, $x_{HS} = (A_3 + A_4)/(A_2 + A_3 + A_4)$, which results in x_{HS} × 100% = 25%. The next spectrum was measured at 400 K. Now, the signal of nitroprusside was totally suppressed, and the LS state absorption was found to be expressed by a doublet with parameters of δ_1 = 0.24 mm s^{-1}, ΔE_{Q_1} = 0.97 mm s^{-1} and two doublets with δ_2 = 0.76 mm s^{-1}, ΔE_{Q_2} = 1.50 mm s^{-1} and δ_3 = 0.95 mm s^{-1}, ΔE_{Q_3} = 2.25 mm s^{-1}, which are assigned to the HS states of $[Fe(abpt)_2]^{2+}$. Then, $x_{HS} = (A_2 + A_3)/\sum A_i$ = 93%. The observed lowered values of the isomer shifts at

dx.doi.org/10.1021/ic201702j | Inorg. Chem. 2011, 50, 12390−12392

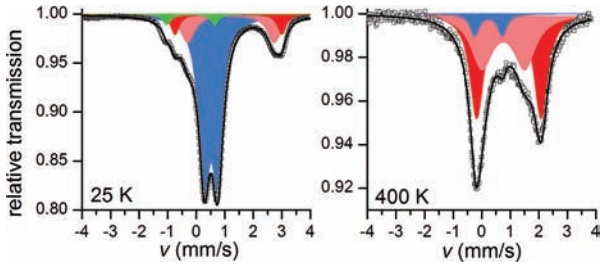

Figure 4. ^{57}Fe Mössbauer spectra for **1′** measured at T = 25 K (left) and 400 K (right). Experimental data: empty squares. Calculated data: full lines. Calculated doublets of pentacyanidonitrosylferrate: green. Calculated doublets of LS and HS iron(II) in $[Fe(abpt)_2]^{2+}$: blue and red (pink), respectively.

elevated temperature can be explained by the second-order Doppler effect[14] and are comparable to the parameters found for $[Fe(abpt)_2(\mu\text{-}Ni(CN)_4)]_n$.[10b] The coexistence of two HS doublets in the isotopically enriched sample can be explained by the presence of structural deformations and different distributions of ^{57}Fe in the solid state. The latter may be supported by a comparison of the Mössbauer spectra of **1** and **1′** measured at 25 K (Figure S5 in the SI). This distribution of HS absorption was found to be much more pronounced in the isotopically enriched $[^{57}Fe(abpt)_2(\mu\text{-}Pt(CN)_6)]_n$ (**2′**) at different temperatures ranging from 5 to 440 K, as discussed in detail in the SI (Figure S6). The course of x_{HS} from the Mössbauer spectroscopy of both compounds copies the main features acquired by magnetic data analysis, which are the existence of a residual HS fraction at low temperature and a residual LS fraction at the highest temperature. However, the exact values are somewhat different as a result of neglect of the divergence of the Lamb−Mössbauer factors and their temperature dependence for each of the present iron(II) ions in the studied compounds.

With the aim of elucidating the role of dianionic polycyanidometallates (PCMs) in the $[Fe(abpt)_2(\mu\text{-}PCM)]_n$ series on the SCO phenomenon, the compounds with tetracyanidopalladate(II) (**3**) and tetracyanidoplatinate(II) (**4**) were also synthesized (see the SI). By a comparison of the magnetic properties of the whole series (Figure S7 in the SI), the shift of the SCO critical temperature T_c was observed in the sequence of $[Fe(CN)_5(NO)]^{2-}$ < $[Pt(CN)_6)]^{2-}$ < $[Ni(CN)_4)]^{2-}$ ≈ $[Pd(CN)_4)]^{2-}$ ≈ $[Pt(CN)_4)]^{2-}$. Then, we can conclude that principally the number of cyanido ligands and the geometry of PCM (square-planar vs octahedral) are crucial aspects of the variation of T_c. Thus, the outcome of this work can serve as a hint to finely tune T_c in other SCO systems analogously as a series of monoanionic pseudohalides or polynitriles.

■ ASSOCIATED CONTENT

Supporting Information

X-ray structure details, calculation details of magnetic data and Mössbauer analyses, and experimental procedures. This material is available free of charge via the Internet at http://pubs.acs.org.

■ AUTHOR INFORMATION

Corresponding Author

*E-mail: zdenek.travnicek@upol.cz.

■ ACKNOWLEDGMENTS

We acknowledge financial support from the Czech Science Foundations (Grants GAČR 203/09/P370, P207/11/0841, and KAN 115600801), and the VaVPI and OPVK projects (Grants CZ.1.05/2.1.00/03.0058 and CZ.1.07/2.3.00/20.0017). The authors thank Jan Filip for PXRD experiments and Libor Machala for help with the fitting of Mössbauer data.

■ REFERENCES

(1) Gütlich, P.; Goodwin, H. A. *Top. Curr. Chem.* **2004**, 233−235.
(2) (a) Fukuda, Y., Ed. *Inorganic Chromotropism*; Springer-Verlag: Berlin, 2007. (b) Gütlich, P.; Hauser, A. *Coord. Chem. Rev.* **1990**, *97*, 1−22. (c) Gütlich, P.; Ksenofontov, V.; Gaspar, A. B. *Coord. Chem. Rev.* **2005**, *249*, 1811−1829. (d) Cannizzo, A.; Milne, C. J.; Consani, C.; Gawelda, W.; Bressler, C.; van Mourik, F.; Chergui, M. *Coord. Chem. Rev.* **2010**, *254*, 2677−2686.
(3) (a) Kahn, O. *Curr. Opin. Solid State Mater. Sci.* **1996**, *1*, 547−554. (b) Gaspar, A. B.; Ksenofontov, V.; Seredyuk, M.; Gütlich, P. *Coord. Chem. Rev.* **2005**, *249*, 2661−2676. (c) Sato, O.; Tao, J.; Zhang, Y. Z. *Angew. Chem., Int. Ed.* **2007**, *46*, 2152−2187.
(4) See, e.g.: (a) Volatron, F.; Catala, L.; Rivière, E.; Gloter, A.; Stéphan, O.; Mallah, T. *Inorg. Chem.* **2008**, *47*, 6584−6586. (b) Agustí, G.; Cobo, S.; Gaspar, A. B.; Molnár, G. b.; Moussa, N. O.; Szilágyi, P. Á.; Pálfi, V.; Vieu, C.; Carmen Muñoz, M.; Real, J. A.; Bousseksou, A. *Chem. Mater.* **2008**, *20*, 6721−6732. (c) Galán-Mascarós, J. R.; Coronado, E.; Forment-Aliaga, A.; Monrabal-Capilla, M.; Pinilla-Cienfuegos, E.; Ceolin, M. *Inorg. Chem.* **2010**, *49*, 5706−5714. (d) Bousseksou, A.; Molnar, G.; Salmon, L.; Nicolazzi, W. *Chem. Soc. Rev.* **2011**, *40*, 3313−3335.
(5) (a) Muñoz, M. C.; Real, J. A. *Coord. Chem. Rev.* **2011**, *255*, 2068−2093. (b) Herchel, R.; Boča, R.; Gembický, M.; Kožíšek, J.; Renz, F. *Inorg. Chem.* **2004**, *43*, 4103−4105. (c) Coronado, E.; Giménez-López, M. C.; Levchenko, G.; Romero, F. M.; García-Baonza, V.; Milner, A.; Paz-Pasternak, M. *J. Am. Chem. Soc.* **2005**, *127*, 4580−4581. (d) Yamauchi, T.; Nakamura, A.; Moritomo, Y.; Hozumi, T.; Hashimoto, K.; Ohkoshi, S. *Phys. Rev. B* **2005**, *72*, 214425. (e) Coronado, E.; Giménez-López, M. C.; Korzeniak, T.; Levchenko, G.; Romero, F. M.; Segura, A.; García-Baonza, V. n.; Cezar, J. C.; de Groot, F. M. F.; Milner, A.; Paz-Pasternak, M. *J. Am. Chem. Soc.* **2008**, *130*, 15519−15532. (f) Maurin, I.; Chernyshov, D.; Varret, F.; Bleuzen, A.; Tokoro, H.; Hashimoto, K.; Ohkoshi, S. *Phys. Rev. B* **2009**, *79*, 064420.
(6) (a) Boča, R.; Nemec, I.; Šalitroš, I.; Pavlík, J.; Herchel, R.; Renz, F. *Pure Appl. Chem.* **2009**, *81*, 1357−1383. (b) Šalitroš, I.; Boča, R.; Dlháň, L.; Gembický, M.; Kožíšek, J.; Linares, J.; Moncol, J.; Nemec, I.; Perašínová, L.; Renz, F.; Svoboda, I.; Fuess, H. *Eur. J. Inorg. Chem.* **2009**, 3141−3154.
(7) Babkov, A. V.; Kharitonov, Y. Y. *Russ. J. Inorg. Chem.* **1999**, *44*, 1749−1763.
(8) See the SI for the synthesis and characterization of **1**−**4**, **1′**, and **2′** in detail.
(9) Kitchen, J. A.; Brooker, S. *Coord. Chem. Rev.* **2008**, *252*, 2072−2092.
(10) (a) Dupouy, G.; Marchivie, M.; Triki, S.; Sala-Pala, J.; Gomez-Garcia, C. J.; Pillet, S.; Lecomte, C.; Letard, J. F. *Chem. Commun.* **2009**, 3404−3406. (b) Herchel, R.; Trávníček, Z.; Zbořil, R. *Inorg. Chim. Acta* **2011**, *365*, 458−461.
(11) Boča, R. *Coord. Chem. Rev.* **2004**, *248*, 757−815.
(12) (a) Bari, R. A.; Sivardie, J. *Phys. Rev. B* **1972**, *5*, 4466−4471. (b) Wajnflas, J. *Phys. Status Solidi* **1970**, *40*, 537−545. (c) Boča, R.; Linert, W. *Monatsh. Chem.* **2003**, *134*, 199−216. (d) Calculation details are presented in the SI.
(13) Goel, P. S.; Garg, A. N. *Inorg. Chem.* **1971**, *10*, 1344−1347.
(14) (a) Greenwood, N. N.; Gibb, T. C. *Mössbauer Spectroscopy*; Chapman and Hall Ltd.: London, 1971. (b) Gütlich, P.; Bill, E.; Trautwein, A. X. *Mössbauer Spectroscopy and Transition Metal Chemistry*; Springer-Verlag: Berlin, 2011.